Computational and experimental study of laminar flames from forest fuels

Computational and experimental study of laminar flames from forest fuels

Virginie Tihay, Albert Simeoni, Paul-Antoine Santoni and Lucile Rossi
SPE – UMR 6134 CNRS
University of Corsica, Campus Grossetti, B.P. 52
20250 Corte
FRANCE
tihay@univ-corse.fr, simeoni@univ-corse.fr, santoni@univ-corse.fr and *lrossi@univ-corse.fr*

Abstract – **Experiments and simulations have been conducted to study the burning of three different vegetative fuels involved in forest fires. An experimental apparatus was designed to generate, in laboratory conditions, laminar, axisymmetric, time-varying and non-premixed flames of these fuels. Characterization of temperature in such flame was managed. The experimental data were used for the testing of a very simple formulation for fuel oxidation. To proceed, the gases released from the pyrolysis of one of the above vegetative fuels were analysed by means of a tube furnace apparatus connected to a gas chromatograph. Using numerical methods the transient equations for the conservation of mass, momentum, energy and chemical species were solved for the flame as well as the radiative transfer equation. The calculated distribution of temperature is presented for this fuel. It does agree with the experimental data recorded as a function of time, at different heights in the flame.**

I. INTRODUCTION

Devastating forest fires regularly damage all continents over the world. It would be very useful to have a predictive tool that can be used for management. The scientific community has become increasingly involved in both modelling and experimental areas. Beginning in North America and Australia fifty years ago [1,2], three types of modelling approaches have emerged. The first one includes statistical models [2]. The second one incorporates empirical models [3]. Based on a detailed description of the heat transfer mechanisms, which govern the fire propagation, the physical models [4-6] are the third set of models. Among them, the two-phase models consider a gas phase flowing through a bed of fuel particles. However, the modelling of the gas fuel combustion has received very little attention. Generally, the combustible part of the devolatilization products is assumed to be only carbon monoxide burning in air [6], whatever vegetation species. Global rate and thermodynamic parameters are included in the model for this representative fuel and oxidizer pair. According to the complexity of plants, the composition of the degradation gases changes with different vegetative species [7].

The effective variability in the amount and composition of these gases as well as the need for a simple reliable model [8] for their oxidation to be included in a model of wildand fire has motivated this work. The structure of an unsteady, axisymmetric, non-premixed laminar flame of pine needles is investigated computationally and experimentally. An experimental device was built in order to generate such a flame. Experimentally, the mass loss and the distribution of temperature along the fire plume are measured and compared for needles from three different pine species. A tube furnace connected to a gas chromatograph allows determining the gases released by the degradation of the needles for one pine species. A simple formulation for fuel oxidation is also provided. A primitive variable formulation was used to solve the transient conservation equations of mass, momentum, energy, species as well as radiation. Predicted and measured temperature along the flame axis was compared at different times during the decreasing flame activity for one of the fuels investigated. The experimental procedures are described in the following section. Next, the numerical method are presented. Finally, the results are discussed.

II. EXPERIMENTAL DEVICES AND METHODS

A. Analysis of the pyrolysis gases

The tube furnace apparatus used as pyrolyser is made of a cylindrical furnace 43.5 cm long with an internal diameter of 6.5 cm. The reactor inside, is 86 cm long with an inner diameter of 5 cm. Experiments were conducted with needles of *Pinus laricius*, an endemic pine of Corsica. Before experiments, pine needles were oven dried at 60°C for 24 hours. Fuel was then crushed and sieved to a particle size of 0.6-0.8 mm. A thermocouple was placed inside the sample to record its temperature history. Two ranges of temperature were used to pyrolyse the fuel: 290 to 425°C and 500 to 600°C. The gas released by the sample at theses ranges of temperature were collected into a gas sampler which was directly attached to gas chromatograph (Flame Ionization Detector and Thermal Conductivity Detector).

B. Time-varying, axisymmetric, diffusion flame

The experimental device is shown in Fig. 1. The bench of combustion was composed of a one square meter plate drilled at its centre. A ten square centimetres insulator was included at this location to support the fuel. It was positioned on a load cell to measure the fuel mass loss as a function of time. A small amount of ethanol (0.3 mL) was spread uniformly on the fuel bed and was ignited with a flame torch to insure a fast and homogeneous ignition. A refined study was conducted to achieve a size and a shape for the fuel bed as well as a size for the particles to be burned, allowing to generate a time-varying, axisymmetric, and laminar diffusion flame. An array of 11 thermocouples was positioned above the fuel bed along the flame axis. The first thermocouple was placed at 1 cm above the top of the support and the others

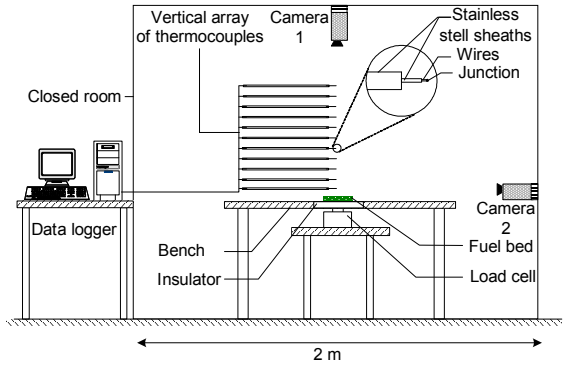

Fig. 1. Sketch of the experimental apparatus.

were located 1 cm from each other. The thermocouples used were mineral–insulated integrally metal-sheathed pre-welded type K (chromel-alumel) pairs of wire with an exposed junction. At the exposed junctions the wires were 50 µm in diameter. The load cell was chosen for his very short response time (0.2 s). The sampling frequency was 100 Hz. The uncertainty in temperature and mass measurements were respectively 0.5°C and 0.1 g. A visual camera located on the side showed that the device effect on the hydrodynamics was negligible. This camera allowed determining the height of the flame too. A second visual camera was placed above the flame in order to study the regression of the flame basis. Thanks to this device, the visual flame height and the visual flame radius are observed what allows comparing the flame behaviour of the three samples. Burnings were conducted with three different types of oven-dried and crushed pine needles from *Pinus laricius*, *Pinus halepensis* and *Pinus pinaster* (all particles sizes of 0.6-0.8 mm). The beds of fuel were in the shape of a disk with a diameter of 3.5 cm, a depth of 0.5 mm and a mass of 1.5 g.

III. NUMERICAL SOLUTION

As this paper is focused on the gas oxidation, the combustion of the vegetative fuel is simplified: the gas and solid phase's interchanges are not considered and the rate of the degradation products entering the gas phase is modelled by a burner. The simulations are made thanks to the software Fluent©. The numerical model solves the two-dimensional, axisymmetric, time-dependent, reactive-flow Navier-Stokes equations coupled with radiation and transport. An ideal gas mixing law defines the viscosity and the thermal conductivity of the mixture. The diffusion coefficients are computed using the kinetic theory [9]. A mixing law defines the specific heat of the mixture. The scattering is neglected in the Radiative Transfer Equation (RTE). To obtain a simple model for radiation, the gas is approximated by a mixture of grey gases containing CO_2 and H_2O. The RTE is solved by using the Discrete Ordinates Method (DOM) [10]. The studied domain is discretized in 8 control angles. Global reactions based on Arrhenius laws were used for CH_4 and CO in order to simplify the combustion of the degradation gases. A single step mechanism was considered for the combustion of CO and a two-step mechanism was used for CH_4. The second step for CH_4 corresponds to the combustion of CO only. Table 1 gives the global reaction rates R where T is the temperature. The kinetic parameters was determined according to [11]. However, the activation energy of this last reaction was fitted to take into account to the laminar pattern of the flow.

IV. RESULTS AND DISCUSSION

A. Degradation of Pinus laricius' needles in the tube furnace

Table 2 shows the main degradation gases analysed for the two ranges of temperature. Degradation gases are mainly made up of CO_2, CO, CH_4, O_2 and lower amounts of H_2, C_2, C_3 and C_4 hydrocarbons. At low temperatures (below 425°C) CO_2 and CO are the main components and represent respectively 79.7% and 13.6% of the whole gases. They arise from the degradation of the extractives, the hemicellulose and from the first stage of the degradation of cellulose [12]. As the temperature attains 500°C, a significant change in the composition of the degradation gases appears. The mass fraction of CO_2 decreases. Conversely the mass fractions of CO, CH_4 and O_2 increase. At this temperature, cellulose, hemicellulose and lignin degrade. Nevertheless, cellulose and hemicellulose are at the end of their degradation stage whereas lignin attains its fastest rate of degradation. Lignin seems to be responsible for the increase in O_2 between the two ranges.

TABLE 1. GLOBAL REACTIONS USED FOR THE COMBUSTION OF THE DEGRADATION GASES IN AIR (UNITS ARE KMOLES, CUBIC METERS, SECONDS AND KELVINS;)

$CH_4 + 1.5\,O_2 \Rightarrow CO + 2\,H_2O$
$R = 5.012\times10^{11}\exp(-24358/T)[CH_4]^{0.7}[O_2]^{0.8}$
$CO + 0.5\,O_2 \Rightarrow CO_2$
$R = 2.239\times10^{12}\exp(-6495/T)[CO][H_2O]^{0.5}[O_2]^{0.25}$

TABLE 2. MASS FRACTIONS OF THE MAIN PYROLYSIS GASES RELEASED BY THE PINUS LARICIUS NEEDLES

	Range of temperature (°C)	
	290–425	500–600
Species	Mass fraction	
O_2	0.029	0.124
CO	0.136	0.2
CO_2	0.797	0.424
CH_4	0.014	0.099
C_2H_4	0.004	0.04
C_2H_6	0.005	0.03
C_3H_6	0.004	0.041
C_3H_8	0.005	0.009
C_4H_8	0.002	0
C_4H_{10}	0.004	0.002
H_2	$1.7\text{x}10^{-4}$	$5.4\text{x}10^{-3}$

B. Burning experiments

Several runs were conducted in Corsica in an enclosure avoiding air motion. The ambient temperature ranged between 21 to 22°C and the relative humidity varied from 50 to 51%. The flame behaviour, the distribution of the vertical temperature along the flame axis, the mass loss as well as the geometry of the flame (radius and height of flame) are discussed hereafter. The mass loss, the mean temperature at the top of the fuel bed and the radius of the flame basis were used to implement the model. The vertical temperatures were used to test the model.

1) Flame behaviour

Figures 2 show the laminar flame of two species, 90 s after the ignition. The flame of *Pinus halepensis* is totally orange that makes it very bright. On the contrary, the flame of *Pinus pinaster* is completely transparent with some blue near the sample. *Pinus laricius* has an intermediate behaviour (and is not provided), since we observe a blue region near the sample followed by an orange-yellow one on the top of the flame. The ability of *Pinus halepensis* to make soot may be higher than *Pinus laricius* and *Pinus pinaster* as flame brightness is related to soot radiation. The same global behaviour was observed for all the pine species, including three different stages: ignition stage, laminar stage and extinction stage. The first stage corresponds to a low turbulent and flickering activity of the flame, showing a clear dominant frequency of about 7 Hz. This behavior was due to the presence of ethanol for ignition. During the second stage, the ethanol was completely burned. The single source of combustible gases was the degradation of pine needles. The flame became laminar (cf. Fig. 2) and decreased slowly. The last stage concerned the extinction of the flame. The remaining solid phase was essentially composed of the carbon skeleton at the surface of the sample as well as a certain amount of unburned fuel near the supporting device. A small (and negligible) amount of ashes at the surface is also observed.

2) Flame height

Figure 3 presents a slow decrease of the height of flame from ignition to extinction for the three species. During the main part of the laminar stage, the *Pinus halepensis* gives the highest flame followed by *Pinus pinaster* and *Pinus laricius*, respectively. This tendency remains valid up to 150 s when it reverses with a low flame. Nevertheless, for *Pinus laricius*, the residence time of the low flame is longer. The heat seems to be diffused deeper in the fuel bed.

3) Flame Radius

During the laminar stage, the mean radiuses of the flame basis were extrapolated for the three pines with quadratic polynomials. These polynomials are used in the simulation for setting the radius of the mass flow inlet zone. The flame

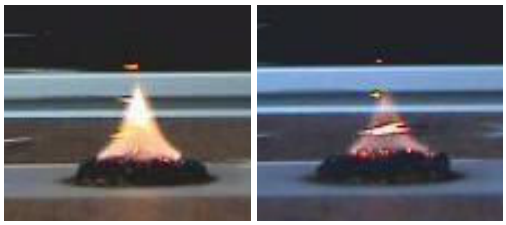

Fig. 2. Flame shape at 90 s a) Pinus halepensis b) Pinus pinaster

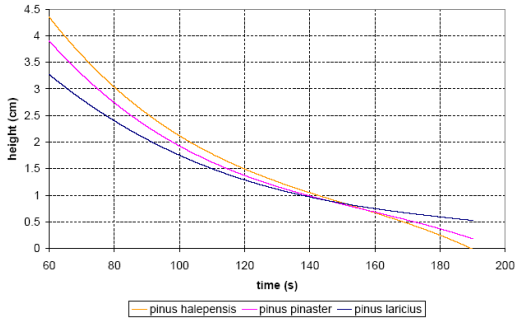

Fig. 3. Mean heights of flames for the three pines.

bases of *Pinus halepensis* and *Pinus pinaster* regress almost in the same way whereas the *Pinus laricius* regresses faster.

4) Mass loss

For the three pines, the mean data provided by the load cell were extrapolated thanks to 4th order polynomials, which are used in the simulation to set the mass flow inlet of degradation gases. During the laminar flame stage, *Pinus halepensis* had the steepest slope followed by *Pinus laricius* and *Pinus pinaster*. After extinction, *pinus pinaster*, *pinus laricius* and *pinus halepensis* lost respectively 0.18, 0.25 and 0.27 g, which corresponds to a global mass losses of 12, 16.7 and 18 %. These low values are due to the compactness of the crushed pine needles bed, avoiding the heat and/or oxygen diffusion through the fuel bed.

5) Vertical temperature

The vertical temperature follows the same trend for the three species. The mean time evolution of the temperatures for vertical thermocouples number 1, 2, 3, 4 and 7 are presented for *Pinus halepensis*, as they are representative of the fire plume (cf. Fig. 4). The first stage of the flame (presence of alcohol) lasts approximately 60 s and is not considered. The second stage corresponds to a typical laminar diffusion flame in which the flame and the thermal plume can be distinguished. During this stage, the first three thermocouples take place inside the laminar flame, while the others are located above it. The temperature in the lower part is maximum reaching 1010°C for thermocouples 1, 2 and 3. In the plume zone (above Th. 4), the temperature decreases progressively from 880°C to the ambient and the flow becomes slightly turbulent. Although the global behaviour is the same for the whole species, some discrepancies are

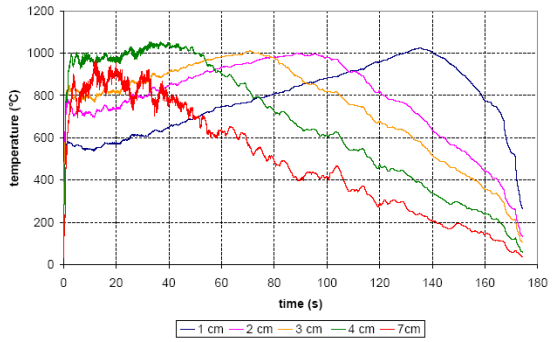

Fig. 4. Mean temperatures along the flame axis for Pinus halepensis.

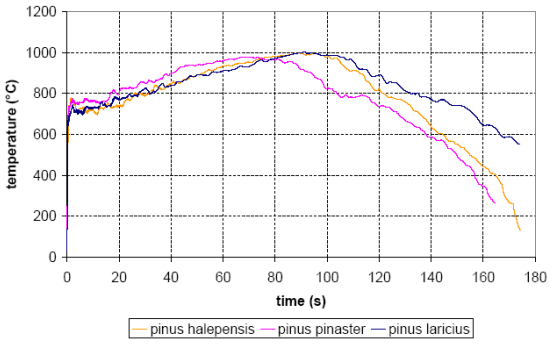

Fig. 5. Mean temperature at 2 cm above the samples for the three pines.

observed. The mean temperature curves at 2 cm, corresponding to the laminar flame are discussed for the three pine species (cf. Fig. 5). *Pinus laricius* and *Pinus halepensis* reach approximately the same temperature about 1000°C, whereas the temperature of *Pinus pinaster* is 25°C lower. *Pinus pinaster* curve increases and decreases more rapidly than the others. The *Pinus laricius* and *Pinus halepensis* follow the same temperature increase but *Pinus laricius* burns longer. These discrepancies are linked to the different mass losses discussed previously.

C. Computational domain and boundary conditions

All the computations have been carried out using a Cartesian non-uniform grid with a width of 6 cm and a height of 15 cm. Two gas mixtures were tested in this study (see Table 3). The values obtained in the tube furnace for the range of temperature 290–425 were used to define them. Thermocouples located inside the fuel bed showed that the needles' temperature was most of the time lower than 425°C. The first mixture only considers CO as combustible gas whereas the second mixture consists of CO and CH_4. For both mixtures, the mass fraction of CO_2 is taken to set the sum of all mass fractions equal to 1.

TABLE 3. MASS FRACTIONS OF THE DIFFERENT SPECIES AT THE BURNER OUTLET FOR THE TWO MIXTURES TESTED

Mixture n°	Y_{CO}	Y_{CH_4}	Y_{O_2}	Y_{CO_2}
1	0.138	0	0.029	0.833
2	0.138	0.014	0.029	0.819

D. Comparison between experimental and numerical results

Figures 6 and 7 show the simulated and experimental temperature during the regression stage, respectively at 2 and 7 cm height. The numerical results correspond to the mixtures of degradation gases given in Table 3. Experimental data were collected from five runs. The decrease of the experimental temperature with time is due to the decrease of the flame. The simulated results present different behaviors for both mixtures in the flame region (Fig. 6). These differences vanish in the thermal plume where the gases are carried out without reaction (Fig. 7). At a height of 2 cm (Figs. 6), the simulated temperature obtained for mixture two, containing CO and CH_4, is roughly in agreement with experiment. Mixture one, containing solely CO underestimates the experimental temperature. The second step in the mechanism of combustion for mixture two makes CO to burn higher along the flame axis than for the one step mechanism used for mixture one. In that case CO burns very close to the burner outlet. From the height of 4 cm, the experimental temperatures diminish drastically over the regression stage (more than 300°C at 4 cm high for instance). This region corresponds to the beginning of the thermal plume. All the predicted curves are close to the experimental ones. Fig. 7 only provides the results at 7 cm high to shorten the presentation. All simulated curves are slightly higher than the experimental ones. These discrepancies could be due to two simplified modeling hypothesis. Firstly, only radiant heat losses due to CO_2 and H_2O were considered. Soot formation/oxidation was not taken into account. Secondly, the model is laminar on the whole domain, whereas the thermal plume becomes turbulent with height. The cooling of the fire plume due to entrainment and mixing of ambient air in the upper part may thus be underestimated in comparison with the experiments. In spite of this discrepancy, simulated and experimental curves follow accurately the same tendency. Considering the whole set of data, the results of simulation for the mixture of CH_4, CO, CO_2 and O_2 match better the experimental data than those resulting from the other mixture without methane (CO, CO_2 and O_2). This first result demonstrates the need to include more species than CO in the global reactions mechanisms used in the two-phase models of wildland fire. These results must be confirmed by further studies.

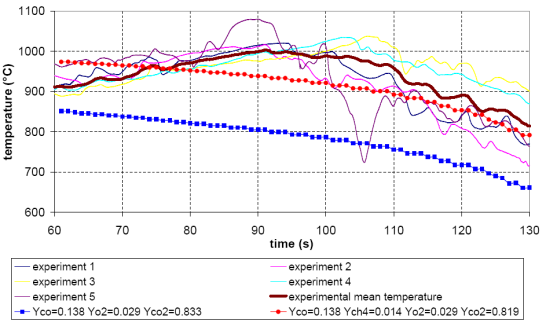

Fig. 6. Observed and simulated temperature in function of time at a height of 2 cm.

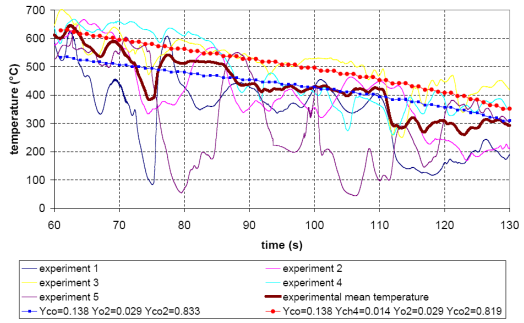

Fig. 7. Observed and simulated temperature in function of time at a height of 7 cm.

V. CONCLUSIONS

From the experimental point of view, the discrepancies between the burning of pine needles litters were previously attributed to the different surface-to-volume ratios of each species [13]. According to our results, this behaviour is also due to the various compositions of the degradation gases, since the discrepancies occur with crushed samples too. This work will be carried on to determine the composition of the degradation gases of other pine species investigated here. From the numerical point of view, the results are encouraging since the simulated temperatures along the flame axis match the observed ones. This work represents the first step for the integration of a gas oxidation model in a wildland fire modeling. Further studies are necessary to test this model for different fuels, both in laminar and turbulent condition, for static and spreading flames. The kinetic of degradation of the solid phase must be investigated too, to take into account the coupling between the flame structure and the solid phase.

VI. REFERENCES

[1] G.M. Byram, in: K. P. Davis (Ed.), *Forest fire control and use*, McGraw-Hill Book Company, New York, 1959, p. 61.

[2] A.G. McArthur, *Weather and grassland fire behaviour*, Leafter n°100, Australian Forest and Timber Bureau, 1966.

[3] R.C. Rothermel, *A mathematical model for predicting fire spread in wildland fuels*, INT-115, USDA Forest Service, 1972.

[4] F.A. Albini, "A model for fire spread in wildland fuels by radiation", *Combust. Sci. Tech.*, 42, pp. 229-258, 1985.

[5] P.A.Santoni, J.H. Balbi, "Modelling of two-dimensional flame spread across a sloping fuel bed", *Fire Safety J.*, 31, pp. 201-225, 1998.

[6] B. Porterie, D. Morvan, J.C. Loraud, M. Larini, "Firespread through fuel beds: Modelling of wind aided fires and induced hydrodynamics", *Phys. Fluids*, 12, pp. 1762-1781, 2000.

[7] W. Klose, S. Damm, W. Wiest, "Pyrolysis and activation of different woods – Thermal analysis (TG/EGA) and formal kinetics", *Proc. Int. Symp. of Catal. and Thermochem. Conv. Of Nat. Org. Polym*. 4, pp. 9-17, 2000.

[8] X.Zhou, S. Mahalingam, "Evaluation of reduced mechanism for modeling combustion of pyrolysis gas in wildland fire", *Combust. Sci. and Tech.,* 171, pp. 39-70, 2001.

[9] McGhee, H.A. *Molecular Engineering*., McGraw-Hill, New York, 1991.

[10] Chui, E.H. and Raithby, G.D., "Computation of radiant heat transfer on a nonorthogonal mesh using the finite-volume method", *Num. Heat Trans. Part B*, 23, pp. 269-288, 1993.

[11] Dryer, F.L. and Glassman, I., "High Temperature Oxidation of CO and CH4", *Proc. Combust. Inst.*, 14, 987, 1973.

[12] J.J.M. Orfão, F.J.A. Antunes, J.L. Figueiredo, "Pyrolysis kinetics of lignocellulosic materials – three independent reactions model", *Fuel*, 78, pp. 349-358, 1999.

[13] J.L. Dupuy, J. Maréchal, D. Morvan, "Fires from a cylindrical forest fuel burner: combustion dynamics and flame properties", *Combust. and Flame*, 135, pp. 65-76, 2003.